Transactions of the Materials Research Society of Japan 30[1] 181-186 (2005)

Suppression of Thermal Interface Degradation in High-k Film/Si by Helium

Kouichi Muraoka
Advanced LSI Technology Laboratory, Corporate R&D Center, Toshiba Corporation
8, Shinsugita-cho, Isogo-ku, Yokohama 235-8522, Japan
Fax: 81-45-770-3667, e-mail: muraoka@amc.toshiba.co.jp

Suppression of thermal interface degradation, especially silicidation, in high-k film (ZrO_2, HfO_2) /Si systems by a helium (He) process, which adds He gas during various annealing processes, was demonstrated. The high-k film/SiO_2 /Si thermal interface stability was investigated in terms of ultrahigh vacuum (UHV), N_2, and He gas annealing with controlled oxygen partial pressure (P_{O2}) at 920 °C. A comparison of UHV, N_2, and He annealing with controlled P_{O2} revealed that the optimal P_{O2} ranges in He at which the thermal stability of a layered structure can be achieved are wider than those in UHV and N_2. Moreover, regarding the poly-Si/SiO_2 /high-k film interface, it was found that He through process consisting of low-temperature SiH_4 flow diluted by He and high-pressure He post-annealing is the most effective means of suppressing silicidation, whereas a conventional N_2 through process cannot. These results indicate that high-concentration He atoms are indispensable for the upper poly-Si/SiO_2 interface. It is supposed that many He atoms physically obstruct SiO creation through the quenching of atomic vibration at the SiO_2 /Si interface, thus impeding the first step of the silicidation reaction. In addition, by comparing with SiO_2 single film, it was found that the suppression efficiency of He atoms in a high-k film/SiO_2 /Si system is higher than that in a SiO_2 /Si system. This phenomenon can be rationalized by assuming that the efficiency reflected the degradation-prone site density in the interfacial SiO_2 layer.
Key words: deposition, annealing, suppression of silicidation, helium, high-k film

1. INTRODUCTION

Recently, there have been expectations that high-k films, for example ZrO_2 and HfO_2, with high dielectric constants and sufficient thermodynamic stability on a Si substrate [1], will be applied as alternative gate insulators for sub-100 nm CMOS transistors [2]. However, the thermal interface degradation problem in high-k film/Si systems remains unresolved. Previous experiments have indicated that the following major problems arise when applying a gate process: (1) At the high-k film/Si substrate (Si-sub) interface, interfacial oxide growth due to residual oxygen in annealing ambient causes the increase of equivalent oxide thickness [3-8] and silicidation due to high-temperature annealing (over 900 °C) under ultrahigh vacuum (UHV) or low oxygen partial pressure (P_{O2}) [4,8-14]; (2) At the poly-Si/high-k film interface, interfacial oxide growth and/or silicidation due to poly-Si deposition by SiH_4 gas [11,15] and silicidation due to high-temperature annealing after the Si deposition [4,11,12,15-18]. Regarding silicide formation, many reaction paths of silicidation for ZrO_2 /SiO_2 /Si systems have already been suggested [4,6-9,11,12]. In particular, the author has found that the trigger of silicidation is the contact of ZrO_2, SiO, and Si accompanying disappearance of the interfacial SiO_2 layer due to SiO removal [10]. This report shows that the SiO molecule plays an important role in silicidation.

Afanas'ev and Stesmans have reported that He gas physically obstructs SiO removal through the quenching of atomic vibration at the interfacial SiO_2 layer, thus impeding SiO_2 /Si interface degradation [19-21]. The purpose of this study is to find ways of suppressing these interfacial reactions, especially silicidation, by controlling the deposition and annealing conditions using He gas. Regarding the high-k film /Si-sub and the poly-Si/high-k film interfaces, the author tried to apply high-temperature He/O_2 annealing to the post-annealing process and to the He through process, that is, a combination of low-temperature SiH_4 /He flow and high-pressure He annealing, respectively, to the poly-Si gate process. In addition, we investigated the origin of high suppression efficiency of He atoms in high-k film /Si systems.

2. EXPERIMENTAL PROCEDURES

Experiments were carried out using a UHV chemical vapor deposition (CVD) chamber system, in which high-k film /SiO_2 /Si samples were annealed under UHV ($< 1 \times 10^{-9}$ Torr), SiH_4, ultra-dry N_2 or He gas taken from conventional gas bottles (purity > 99.99998%). N_2 and He were passed through a purifier and a liquid nitrogen trap. With this equipment, partial pressures of residual O_2, H_2O and H_2 can be reduced to less than 1×10^{-9} Torr under N_2 and He ambients. P_{O2} in annealing ambients was controlled in the range of 1×10^{-9} to 1×10^{-4} Torr by using an independent oxygen variable leak valve, and monitored by quadrupole mass spectrometry. In addition, the surface temperatures of the samples were monitored by a pyrometer.

Details of the experimental procedures are given below. CZ n-type Si(100) substrates were cleaned by RCA treatment and 1 nm chemical oxides were grown on Si substrates. Next, ZrO_2 and HfO_2 films (2, 20 nm)

were formed on the chemical oxides by sputtering of ZrO_2 and HfO_2 targets (Ar/O_2 RF plasma 400 W) at room temperature, respectively. This sputtering process causes an increase in interfacial oxide thickness (1 → 3 nm). The samples were then transferred to the UHV-CVD chamber. The samples were made both with and without a poly-Si cap by using the following processes: (1) the samples were annealed at 920 °C for 1-10 min in various P_{O2} under UHV, N_2 or He 1 Torr; (2) Si films (~ 2, ~ 20 nm) were formed on these high-k films using SiH_4 1 Torr diluted by N_2 or He 2 Torr at 500 ~ 650 °C. After the Si deposition, the samples were annealed at 920 °C for 1 min in N_2 or He ranging from 0.1 to 300 Torr. Regarding physical analysis, changes of bonding states and layered structures of high-k film /SiO_2 /Si with and without a poly-Si cap before and after annealing were measured by *in-situ* x-ray photoelectron spectroscopy (*in-situ* XPS) and transmission electron microscopy (TEM), respectively.

3. RESULTS

3.1 High-k Film /Si-sub Interface

It has been reported that the window of optimal P_{O2} is narrow in which the thermal stability of high-k film /SiO_2 /Si structure can be achieved [6-8]. The author investigated these windows under various ambients. Figure 1 shows the changes in Zr3d and Si2p core-level spectra from ZrO_2 /SiO_2 /Si in UHV, N_2, and He ambients with $P_{O2} = 1 \times 10^{-7}$ Torr.

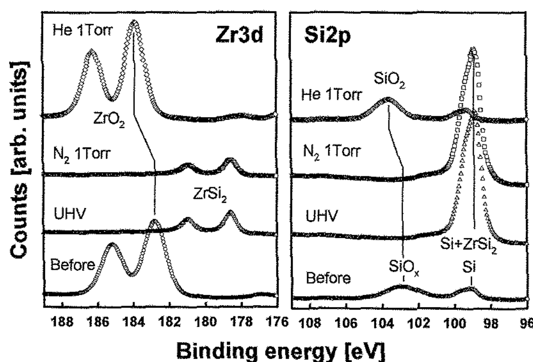

Fig. 1. Changes in Zr3d and Si2p core-level spectra from ZrO_2/SiO_2/Si in various ambients (920 °C 10 min, $P_{O2} = 1\times10^{-7}$ Torr). The x-ray source was MgK_α and the take-off angle of photoelectrons was 45°. Binding energy shifts were compensated by the binding energy of the Si2p peak of silicon substrate (99.2eV).

Regarding Zr3d spectra, it is clearly shown that He gas suppresses silicidation far more effectively than does UHV or N_2 gas. The increase of peak intensity and the decrease of full width at half maximum were caused by the increase of film density and the decrease of variation in bond configuration, respectively. It is notable that the Zr3d peak moved toward higher binding energy after the He annealing. The shift amount of the Zr3d peak is close to that of the chemical shift component of the Si2p spectra (SiO_x → SiO_2). Therefore, the electric charging due to insulating improvement of the ZrO_2 /SiO_2 layer causes band bending of the interfacial SiO_2 layer during XPS measurement [5,22]. A comparison of the Si2p chemical shift component's shape, in addition, revealed that the He annealing changed silicate-like SiO_2 (broad SiO_x peak [5]) into pure SiO_2 (sharp peak), thus causing phase separation but not silicidation at the interface region. These phenomena are also confirmed by the TEM images shown in Fig. 2.

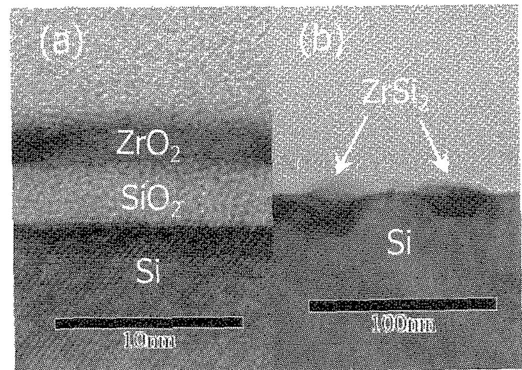

Fig. 2. Cross-sectional TEM images of ZrO_2 /SiO_2 /Si (920 °C 10 min (a) He, (b) N_2 1 Torr, $P_{O2} = 1\times10^{-7}$ Torr). It was confirmed by energy dispersive x-ray spectroscopy that the composite of silicide grain is $ZrSi_2$.

It was confirmed that the ZrO_2 /SiO_2 layered structure remained after He annealing (a). In contrast, the layered structure disappeared, and many silicide ($ZrSi_2$) grains were embedded locally in the Si substrate after N_2 annealing (b), as in the case of UHV annealing [10,12]. The existence of embedded $ZrSi_2$ in Si can explain the results of increased Si2p substrate intensity and decreased SiO_x-Si2p and Zr3d intensities as shown in Fig. 1.

Next, the optimal P_{O2} ranges where the interfacial SiO_2 layer does not grow or disappear (complete silicidation) by He and N_2 annealing were investigated as shown in Fig.3.

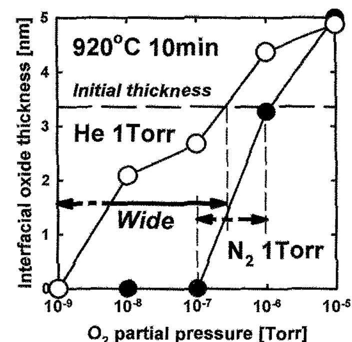

Fig. 3. Interfacial oxide thickness as a function of P_{O2} in annealing ambients. These thicknesses were calculated using Si2p photoelectron escape depth inside SiO_2 (Ref. 23), and were about equal to those obtained by TEM measurement. The arrows denote the optimal P_{O2} ranges where the interfacial SiO_2 layer does not grow or disappear.

It was confirmed that the window of optimal P_{O2} in N_2 ambient is very narrow ($1\times10^{-7} < P_{O2} < 1\times10^{-6}$ Torr) and roughly similar to that reported by Maria [6]. In the

case of He annealing, the stability of the layered structure was demonstrated at $1\times10^{-9} < P_{O2} < 3\times10^{-7}$ Torr, and interfacial oxide thicknesses can be reduced by phase separation and densification at $P_{O2} = 1\times10^{-8} \sim 1\times10^{-7}$ Torr. Thus, the optimal P_{O2} range in He (over 2 orders) is wider than that in N_2 (just 1 order). It is an interesting point that the interfacial oxide after He annealing is thicker than that after N_2 annealing at $P_{O2} = 1\times10^{-6}$ Torr. The interfacial oxide thickness is thought to increase due to the suppression of SiO desorption in He ambient, whereas the balance of SiO desorption and oxidation by O_2 is maintained in N_2 ambient. Similarly, because the oxidation by O_2 becomes dominant rather than the suppression of SiO desorption, both differences can be expected to disappear at $P_{O2} = 1\times10^{-5}$ Torr.

The optimal P_{O2} regions of various oxide films including $ZrSiO_4$ and SiO_2 [24,25] were also investigated and compared as in the case of ZrO_2 film (Fig. 4).

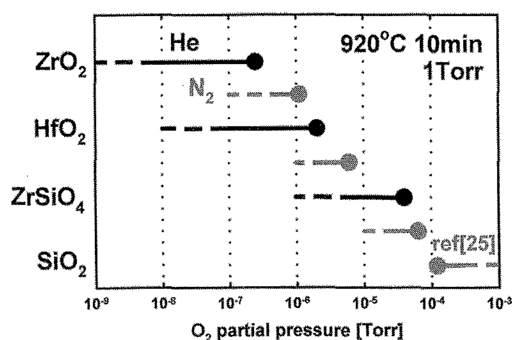

Fig. 4. Optimal O_2 partial pressure regions of various oxide films. The horizontal lines denote the optimal ranges where the interfacial SiO_2 layer does not grow or disappear. Solid circles indicate the boundaries of interfacial SiO_2 growth, and pressures lower than those indicated by the circles are preferable.

It was confirmed that He annealing is also an effective method for the suppression of silicidation for HfO_2 and $ZrSiO_4$ films, and the range of the operating O_2 partial pressure for these oxide films was widened successfully. In addition, a relationship among optimal O_2 partial pressure regions in various oxide films was found ($ZrO_2 < HfO_2 < ZrSiO_4 < SiO_2$). It is thought that the optimal region depends on the balance of SiO desorption and oxidation by atomic oxygen, especially the amount of atomic oxygen created by vacancy in high-k film [26,27]. In the case of ZrO_2 and HfO_2, the difference in kinds of vacancy related to Zr and Hf atoms may cause the difference in the amount of created atomic oxygen. Actually, Quevedo-Lopez has reported that interfacial oxide growth of ZrSiOx is larger than that of HfSiOx [28]. From these results, it is supposed that the amount of atomic oxygen created by ZrO_2 is larger than the amount created by HfO_2. In the case of ZrO_2 and $ZrSiO_4$, the difference in amount of vacancy related to the Zr atom may also cause the difference in the amount of created atomic oxygen. Thus, it is also supposed that the relationship of optimal regions of ZrO_2, $ZrSiO_4$ and SiO_2 reflects the difference in the amount of created atomic oxygen ($ZrO_2 > ZrSiO_4 > SiO_2$). From our experimental results, the author suggests that the origin of the optimal window is decided by the kind and the amount of vacancy in high-k film.

3.2 Poly-Si /High-k Film Interface

In this section, the author investigated the Si deposition and the post-annealing effects, respectively. Figure 5(a) shows the changes in Zr3d spectra from the ZrO_2 (20 nm) surface before and after thin Si-cap deposition by SiH_4/N_2 flow.

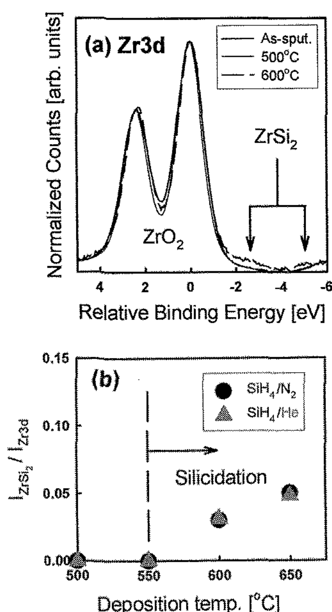

Fig. 5. (a) Changes in Zr3d spectra from ZrO_2 (20 nm) surface before and after SiH_4/N_2 flow; (b) Temperature dependences of silicidation under SiH_4/N_2 and SiH_4/He. The vertical axis is the ratio of $ZrSi_2$ and total Zr3d intensities (shown in (a)).

It is confirmed that there was no change in Zr3d spectra before and after deposition at 500 °C. In contrast, it is clearly shown that deposition at 600 °C causes surface silicidation. This result is similar to that reported by Perkins [11]. The temperature dependences of silicidation under SiH_4/N_2 and SiH_4/He are indicated in Fig.5(b). It is found that the silicidation does not depend on dilution gas and can be suppressed by lowering the initial deposition temperature below 600 °C. Under this condition, the author investigated the interfacial structure of thin Si-cap/ZrO_2 film by using *in-situ* angle-resolved XPS analysis. Figure 6 shows the Si2p spectra from ZrO_2 (20 nm) surface after SiH_4 /He deposition at 500 °C. It can be confirmed that SiO_2 peak of take-off angle (TOA) = 45° is higher than that of TOA = 20°. This result indicates that thin SiO_2 film (~ 0.7 nm) is formed between the Si cap (~ 1.4 nm) and the ZrO_2 surface [29]. Similarly, Jeon has also confirmed this interfacial SiO_2 growth [4]. Moreover, it is confirmed by *in-situ* XPS and thermal desorption spectroscopy analysis that this SiO_2 growth did not occur when the Si cap was deposited on a clean Si surface. The adsorbed H_2O molecules on a ZrO_2 surface have the desorption peak of 350 °C and are almost desorbed at a temperature lower than 500 °C (not shown

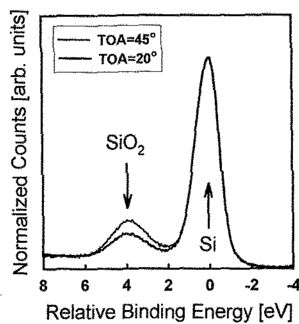

Fig. 6. Si2p spectra from the ZrO_2 (20 nm) surface after SiH_4/He flow (500 °C) as a function of photoelectron TOA.

). Thus, oxygen atoms that compose the SiO_2 layer are not supplied from the adsorbed H_2O but from the lower ZrO_2 film under the Si deposition condition. This result means that the SiH_4 flow causes the formation of oxygen vacancies near the ZrO_2 surface. The author has also investigated the interfacial reaction of HfO_2 [30]. It has been reported that there is no Hf silicide peak below 650 °C and the peak slightly increases at 650 °C. In addition, it has been confirmed that thin SiO_2 (~ 0.8 nm) grows between the Si cap (~ 2.6 nm) and the HfO_2 surface at 600 °C. When the deposition temperature is lowered to 500 °C, although the thickness of the SiO_2 layer decreases to approximately 0.7 nm, it cannot be removed completely. These results are similar to the experimental results of the electron energy loss spectroscopy analysis reported by Wilk and Muller [31], and indicate that the oxygen vacancies are formed near the HfO_2 surface, as is also the case for the ZrO_2 surface. In regard to electrical properties, Kaneko has reported that complex defects of dopant and Hf silicate are localized near the poly-Si/Hf silicate interface with a finite width of approximately 1 nm [32]. This suggests that the oxygen vacancies near high-k film surfaces are the origin of the electrical defects.

The author summarizes the critical condition of silicidation during deposition as follows, which does not depend on dilution gas. Above 600 and 650 °C, SiH_4 flow causes silicidation at ZrO_2 and HfO_2 surfaces, respectively. The experimental results shown in Fig.5(a) and Fig.3(a) of Ref. 30 indicate that the silicide density on ZrO_2 is large compared with that on HfO_2. It is thought that the difference in the ratios of silicidation for ZrO_2 and HfO_2 is based on the difference in mass transports of Zr and Hf atoms [28]. Below 600 and 650 °C, silicidation does not occur, but interfacial oxide grows due to the formation of oxygen vacancy at ZrO_2 and HfO_2 surfaces, respectively.

Next, to investigate the effect of ambient gas during post-annealing, the author prepared the initial structure of the Si cap (~ 1.4 nm)/ SiO_2 (~ 0.7 nm)/ high-k film /SiO_2 (3 nm) /Si formed by deposition at 500 °C without silicidation. Following this, the samples were annealed at 920 °C in N_2 or He ambients at various pressures. Thus, we made the samples with the poly-Si cap by using 4 kinds of processes: SiH_4/N_2 + N_2 (N_2 through process), SiH_4/He + N_2, SiH_4/N_2 + He, and SiH_4/He + He (He through process).

First, we investigated the ambient gas dependence of

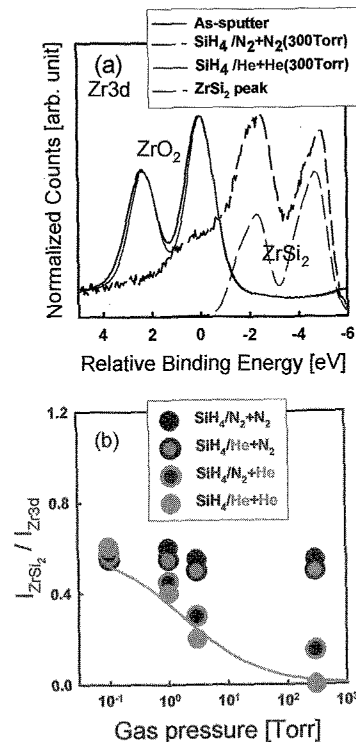

Fig. 7. (a) Changes in Zr3d spectra from the ZrO_2 (2 nm) surface after N_2 and He through processes; (b) Ambient gas and pressure dependences of silicidation. Vertical axis is the same as that in Fig.5(b).

silicidation of ZrO_2. Figure 7(a) shows the changes in the Zr3d spectra from the ZrO_2 (2 nm) surface after applying N_2 and He through processes. $ZrSi_2$ peak [16] is also indicated for comparison. It is found that the He through process can completely suppress the silicidation, as indicated by the gray solid line, whereas the N_2 through process cannot suppress it. Figure 7(b) shows the ambient gas and pressure dependences of silicidation for the 4 kinds of processes. This result reveals two important points. First, higher-pressure He annealing tends to suppress the silicidation. Second, the combination of SiH_4/ He and highest-pressure He annealing is the most effective. These results can also be seen in the TEM images. Figure 8 shows the cross-sectional TEM images of poly-Si (20 nm)/ZrO_2 (2 nm)/SiO_2 /Si after deposition at 500 °C and post-annealing at 300 Torr. The left- and right-hand columns are for the SiH_4 /N_2 and the SiH_4 /He depositions, respectively. Upper and lower lines are for the N_2 and the He annealing, respectively. In the case of N_2 annealing, lower interfacial oxides disappeared locally and large silicide grains embedded in the poly-Si gate (Fig. 8(a), (b)). In contrast, it was confirmed that the interfacial oxides remained after He annealing (Fig. 8(c), (d)). It is noted that a combination of SiH_4/N_2 and He annealing creates small silicide grains in the poly-Si gate (Fig. 8(c)), whereas the He through process does not create them (Fig. 8(d)). We have also investigated the effect of the He through process regarding HfO_2 [30]. It has been reported that the He through process can completely suppress the silicidation, whereas the N_2 through process cannot. Thus, the He through process is effective also for HfO_2.

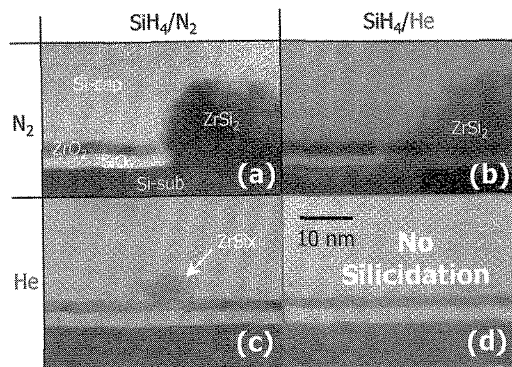

Fig. 8. Cross-sectional TEM images of poly-Si (20 nm) /ZrO_2 (2 nm) /SiO_2 /Si after deposition at 500 °C and post-annealing at 300 Torr; (a) SiH_4 /N_2 + N_2 (N_2 through process); (b) SiH_4 /He + N_2; (c) SiH_4 /N_2 + He; (d) SiH_4 /He + He (He through process).

4. DISCUSSION

Why is He effective in the suppression of interface degradation? Regarding the SiO_2 /Si system, suppression of thermal degradation by He has already been reported by Afanas'ev and Stesmans [21]. In the case that many He atoms exist at the SiO_2 /Si interface, dissipation of vibration energy through multiple He collisions occurs at local defects. By this energy dissipation effect, He annealing causes the suppression of the bond-breaking at the SiO_2 /Si interface. As an example, the pressure dependence of SiO_2 /Si degradation suppression by He has been shown in Ref. 21. As the He gas pressures increase, the increase of positive fixed charge is suppressed. Thus, this result means that high-pressure He annealing is the most effective means of suppressing thermal degradation. Regarding silicidation, the author has already suggested the reaction steps of silicidation and the suppression model by He as follows. Conventional N_2 annealing cannot suppress the bond-breaking and the SiO diffusion at a lower interface, and the silicidation is caused by the contact of high-k film, SiO and poly-Si [24]. In contrast, He annealing can physically obstruct SiO creation at the lower interface due to the dissipation of vibration energy [24,33]. However, the combination of SiH_4 /N_2 and He annealing cannot suppress the silicidation at the upper interface (Fig. 8(c)). There is a possibility that the upper thin SiO_2 film formed by Si-cap deposition is defective and is more easily degraded by SiO creation than the lower thick SiO_2 film. In the case of the He through process, many He atoms can exist in poly-Si, SiO_2 and high-k film. Thus, it is expected that higher-concentration He atoms are indispensable for sufficiently quenching the upper atomic vibration.

Based on the Afanas'ev-Stesmans model, the simulation of the suppression effect for silicidation was performed, taking the results of He gas pressure dependence into consideration (Fig. 7(b)). The efficiency R of He gas blocking action for thermal degradation of the SiO_2/ Si interface is defined from the increase in defect density after annealing under He gas pressure p (ΔN_{He} (p)) and that after annealing in a vacuum (ΔN_{vac}): $R = \Delta N_{vac} / \Delta N_{He}(p) - 1 \propto D(cp)^{2/3}$, where D is the diffusion coefficient and c is the solubility in SiO_2 film at an annealing temperature [21]. When it is assumed that the ratio of silicidation is proportional to the increase in defect density (ΔN), the ratio of silicidation after He annealing under pressure p (I_{ZrSi2} / I_{Zr3d} (p)) is expressed in the equation,

$$\frac{I_{ZrSi_2}}{I_{Zr3d}}(p) = \frac{I_{ZrSi_2}}{I_{Zr3d}}(vac) \times \frac{1}{Ap^{2/3}+1} \quad (1).$$

A is a proportional constant and I_{ZrSi2} / I_{Zr3d} (vac) is the ratio of silicidation after vacuum annealing. It is found that Eq. (1) is in good agreement with the experimental results of the He through process in Fig. 7(b) (gray line which connects the data points). This supports not only the silicidation model that the thermal degradation of SiO_2 /Si interface is the first step of a silicidation reaction [16,24], but also the suppression model that the suppression of microscopic defect formation by high-concentration He atoms causes the suppression of macroscopic silicidation [24,33]. By using the He through process to realize high-concentration He atoms, we can achieve the suppression of degradation at upper and lower interfaces.

Moreover, other important knowledge can be acquired from this experiment. By comparing with SiO_2 single film, it is found that the suppression efficiency R of He 300 Torr in ZrO_2 /SiO_2 /Si system is approximately 31, which is at least 10 or more times that in the SiO_2 /Si system ($R < 3$) [21]. Although compared with other experimental results for SiO_2 in the range from 900 to 1000 °C [20], the suppression effect by He at the ZrO_2 /SiO_2 /Si interface is very large. This phenomenon can be rationalized by presupposing that the proportional constant A in $R = Ap^{2/3}$ reflected the degradation-prone site density N_D in the interfacial SiO_2 layer. Thus, in the case that many sites that easily cause thermal degradation exist in the SiO_2 layer, the collision probability of those sites and He atoms which diffuse in the SiO_2 network, increases in proportion to the site density N_D, i.e., $A \propto N_D$, and it can be expected that R becomes large because A is large in spite of low He pressure. In fact, it has been reported that the thermal stability of SiO_2 film in contact with ZrO_2 film is lower and the fixed charge density in its SiO_2 film is 1 ~ 2 orders higher than that in a SiO_2 single film [10,31,32]. These results support the validity of this model. Thus, this model also indicates that the He through process is more effective in the hetero-interface with high-density degradation-prone sites and low thermal stability.

5. CONCLUSIONS

Suppression of thermal interface degradation, especially silicidation, in high-k film/Si systems by He process in which He gas is added during various annealing processes was demonstrated. Regarding the high-k film /SiO_2 /Si interface, we investigated the thermal interface stability in terms of UHV, N_2, and He gas annealing with controlled P_{O2} at 920 °C. Comparison of UHV, N_2, and He annealing with controlled P_{O2} revealed that the optimal P_{O2} ranges in He at which the thermal stability of the layered structure can be achieved are wider than those in UHV and N_2. Moreover, regarding the poly-Si/SiO_2 /high-k film interface, it is found that the He through process of low-temperature

SiH_4 flow diluted by He and high-pressure He post-annealing is the most effective means of suppressing silicidation, whereas the conventional N_2 through process cannot. These results indicate that high-concentration He atoms are indispensable for the upper poly-Si/SiO_2 interface. It is assumed that many He atoms physically obstruct SiO creation through the quenching of atomic vibration at the SiO_2/Si interface, thus impeding the first step of the silicidation reaction. In comparison with SiO_2 single film, it is found that the suppression efficiency of He atoms in high-k film/SiO_2/Si systems is higher than that in the SiO_2/Si system. This phenomenon can be rationalized by assuming that the efficiency reflected the degradation-prone site density in the interfacial SiO_2 layer.

ACKNOWLEDGMENTS

The author is grateful to K. Kurihara, Y. Mitani, K. Kato, Y. Nakasaki, H. Nishino, I. Kamioka, M. Koyama, and A. Nishiyama for their useful discussions, and to M. Koike and A. Kaneko for help with high-k film sputtering.

REFERENCES

[1] K. J. Hubbard and D. G. Schlom, J. Mater. Res. **11**, 2757 (1996).
[2] G. D. Wilk, R. M. Wallace, and J. M. Anthony, J. Appl. Phys. **89**, 5243 (2001).
[3] M. Copel, M. Gribelyuk, and E. Gusev, Appl. Phys. Lett. **76**, 436 (2000).
[4] T. S. Jeon, J. M. White, and D. L. Kwong, Appl. Phys. Lett. **78**, 368 (2001).
[5] H. Watanabe, Appl. Phys. Lett. **78**, 3803 (2001).
[6] J.-P. Maria, D. Wicaksana, A. I. Kingon, B. Busch, H. Schulte, E. Garfunkel, and T. Gustafsson, J. Appl. Phys. **90**, 3476 (2001).
[7] S. Stemmer, Z. Chen, R. Keding, J.-P. Maria, D. Wicaksana, and A. I. Kingon, J. Appl. Phys. **92**, 82 (2002).
[8] N. Miyata, M. Ichikawa, T. Nabatame, T. Horikawa, and A. Toriumi, Jpn. J. Appl. Phys. **42**, L138 (2003).
[9] J. P. Chang and Y.-S. Lin, Appl. Phys. Lett. **79**, 3824 (2001).
[10] H. Watanabe and N. Ikarashi, Appl. Phys. Lett. **80**, 559 (2002).
[11] C. M. Perkins, B. B. Triplett, P. C. McIntyre, K. C. Saraswat, and E. Shero, Appl. Phys. Lett. **81**, 1417 (2002).
[12] M. A. Gribelyuk, A. Callegari, E. P. Gusev, M. Copel, and D. A. Buchanan, J. Appl. Phys. **92**, 1232 (2002).
[13] M.-H. Cho, Y. S. Roh, C. N. Whang, K. Jeong, S. W. Nahm, D.-H. Ko, J. H. Lee, N. I. Lee, and K. Fujihara, Appl. Phys. Lett. **81**, 472 (2002).
[14] Y.-S. Lin, R. Puthenkovilakam, and J. P. Chang, Appl. Phys. Lett. **81**, 2041 (2002).
[15] K-Y Lim, D-G Park, H-J Cho, J-J Kim, J-M Yang, II-S Choi, I-S Yeo, and J-W Park, J. Appl. Phys. **91**, 414 (2002).
[16] K. Muraoka, Appl. Phys. Lett. **80**, 4516 (2002).
[17] M. Koyama, K. Suguro, C. Hongo, M. Koike, Y. Kamimuta, M. Suzuki, and A. Nishiyama, Mat. Res. Soc. Symp. Proc., **716**, 151 (2002).
[18] Y. Morisaki, T. Aoyama, Y. Sugita, K. Irino, T. Sugii, and T. Nakamura, Tech. Dig. Int. Electron Devices Meet. **2002**, 861.
[19] V. V. Afanas'ev and A. Stesmans, Appl. Phys. Lett. **74**, 1009 (1999).
[20] A. Stesmans, V. V. Afanas'ev, and A. G. Revesz, Appl. Phys. Lett. **74**, 1466 (1999).
[21] V. V. Afanas'ev and A. Stesmans, J. Appl. Phys. **87**, 7338 (2000).
[22] S. Iwata and A. Ishizuka, J. Appl. Phys. **79**, 6653 (1996); K. Muraoka and S. Inumiya, Ext. Abst. Of the 6th Workshop on Formation, Characterization and Reliability of Ultrathin Silicon Oxides, JSAP Catalog No. AP012202, 187 (2001).
[23] Z. H. Lu, J. P. McCaffrey, B. Brar, G. D. Wilk, R. M. Wallace, L. C. Feldman, and S. P. Tay, Appl. Phys. Lett. **71**, 2764 (1997).
[24] K. Muraoka, IEICE Trans. Electron., **E87-C**, 9 (2004).
[25] J. V. Seiple and J. P. Pelz, J. Vac. Sci. Technol. A, 13, 772 (1995).
[26] A. S. Foster, V. B. Sulimov, F. L. Gejo, A. L. Shuluger, and R. M. Nieminen, Phys. Rev. B **64**, 224108-1 (2001).
[27] A. S. Foster, F. Lopez Gejo, A. L. Shluger, and R. M. Nieminen, Phys. Rev. B **65**, 174117-1 (2002).
[28] M. A. Quevedo-Lopez, M. El-Bouanani, B. E. Gnade, R. M. Wallace, M. R. Visokay, M. Douglas, M. J. Bevan, and L. Colombo, J. Appl. Phys. **92**, 3540 (2002).
[29] The thicknesses of the Si-cap and interfacial SiO_2 layer were obtained by analyzing the angle-resolved Si2p spectra, assuming electron escape depths of Si2p for Si and SiO_2 of 2.4 and 3.3 nm, respectively. These escape depths were determined by comparing the Si2p spectra with the thickness of the Si-cap on thick SiO_2 film and the thickness of SiO_2 on Si substrate determined by TEM.
[30] K. Muraoka, J. Appl. Phys. **96**, 2292 (2004).
[31] G. D. Wilk and D. A. Muller, Appl. Phys. Lett. **83**, 3984 (2003).
[32] A. Kaneko, S. Inumiya, K. Sekine, M. Sato, K. Kamimuta, K. Eguchi, and Y. Tsunashima, Ext. Abs. Int. Conf. Solid. State Device and Materials **2003**, 56.
[33] K. Muraoka, Appl. Phys. Lett. **81**, 4171 (2002).

(Received December 23, 2004; Accepted February 3, 2005)